Payri, R.; Gimeno, J.; Carreres, M.; Montiel-Prieto, T. (2021). Understanding the effect of inter-jet spacing on lift-off length and ignition delay. Combustion and Flame. 230:1-12. https://doi.org/10.1016/j.combustflame.2021.111423

Raul Payri, Jaime Gimeno, Marcos Carreres, Tomas Montiel; Understanding the effect of inter-jet spacing on lift-off length and ignition delay; Combustion and Flame, vol. 230, no. August, p. 111423, 2021. DOI: 10.1016/j.combustflame.2021.111423.

Understanding the effect of inter-jet spacing on Lift-off Length and Ignition Delay

Raul Payri[a,*], Jaime Gimeno[a], Marcos Carreres[a], Tomas Montiel[a]

[a] *CMT - Motores Térmicos, Universitat Politècnica de València, Edificio 6D, 46022, Valencia, Spain.*

Abstract

In recent years, injectors with multiple outlet-holes and smaller diameters have been implemented to reduce pollutant emissions during the combustion development. Nevertheless, increasing the number of holes has also decreased the spacing between the jets, which could lead to interactions between sprays affecting their behavior, a phenomenon that has not been defined in detail. In this sense, this study analyzes the influence of inter-jet spacing on the ignition delay and lift-off length for a wide range of boundary conditions. To this end, two multi-hole diesel injectors were manufactured with different distributions of the outlet orifices, which allowed the study of the development of an isolated spray and a spray with an inter-jet spacing of 30° during the same injection event. Additionally, the results were compared to the development of sprays under inter-jet spacing values of 36° and 45°. The results showed that the spray with smaller inter-jet spacing had a slightly larger ignition delay at low chamber temperature and density conditions. Regarding the lift-off length, reducing the inter-jet spacing decreased the lift-off length values, these reductions being more noticeable after a threshold of proximity between sprays was achieved. In particular, the spray with an inter-jet spacing value of 30° had considerably lower lift-off length values than those with an inter-jet spacing of 36° and 45°, which in turn had closer lift-off length values than those obtained with the isolated spray. Finally, a novel empirical correlation was developed for the lift-off

*Corresponding author. E-mail address: rpayri@mot.upv.es

length considering the influence of inter-jet spacing, thus contributing to the understanding of the effect of the interaction between sprays in the combustion process.

Keywords: Lift-off length, ignition delay, inter-jet spacing, diesel injection

1. Introduction

The rise in popularity of internal combustion engines in the last decades and the rising environmental awareness, have led to the creation of emissions and fuel economy legislations that have been increasingly restrictive throughout the years [1]. These events have motivated researchers to continuously search for improvements in multiple areas of the internal combustion engine [2, 3].

Regarding the diesel injection event, injectors with multiple holes have been established as one of the numerous techniques employed in modern diesel engines to reduce its emissions [4]. In this sense, the incrementation of the number of outlet holes has allowed for smaller diameter of these holes, leading to more homogeneous mixtures and smaller droplet sizes, enlarging the liquid-gas contact surface. These phenomena have enhanced the injection event [5], as the mixing process is crucial for the combustion efficiency [6].

Nevertheless, as the number of holes in the nozzle increases, the spacing between them decreases, leading to a reduction in the space available for each jet to develop without interacting with the neighbor sprays. Then, increasing the number of holes presents a trade-off between improving the air entrainment through smaller orifices diameter, and providing a bigger volume of air between the sprays. In this sense, as the sprays come closer between each other, jet-to-jet interaction could have a significant effect on the combustion process. This phenomenon is a matter of interest among the research community, as its implications have not been entirely defined [7, 8].

Rusly et al. [9] investigated the development of wall-interacting jets and jet-jet interaction in a small-bore optical diesel engine. They found that, for narrow

inter-jet spacing, the impact of jet-jet interaction on the lift-off length and higher soot formation is more significant than the effect of the re-entrainment, due to rich mixture formed in-between jets. To avoid an increase on soot formation, the authors suggested the implementation of split injections and larger bowl diameter, as well as increasing the inter-jet spacing to reduce the high-temperature gas re-entrainment and shorten of the lift-off length. Similar results were found by Le et al. [10].

Chartier et al. [11] conducted lift-off measurements in an optical heavy-duty diesel engine, using various hardware configurations in order to investigate the influence of jet-jet interactions on the lift-off length. They indicated that burned gases from neighbor jets are entrained in the lift-off region, shortening the lift-off length. They also stated that this phenomenon gained importance when reducing the inter-jet spacing. Additionally, the authors found a strong interaction between the chamber gas temperature and the spacing between jets. Specifically, their results stated that, for closer inter-jet spacing, the chamber temperature had a considerably lower influence on the lift-off length variations, in contrast with its impact for large inter-jet spacing conditions. A plausible explanation noted by the authors is that the local gas temperature experienced by the jet, at close inter-jet conditions, is dominated by the re-entrained burned gas.

Moreover, Lequien et al. [12] studied the liquid length under reacting conditions in an optical heavy-duty DI diesel engine. The authors noticed a shorter liquid length penetration for the spray with maximum inter-jet spacing, finding that the hot gas reservoirs formed by the combustion products near the lift-off area were not strongly influencing the liquid length. Moreover, the authors attributed this trend to the cooling effect of the surrounding jets.

The mentioned works were performed in real diesel engines, in which minor modifications were done to gain optical access to the combustion chamber. These studies are important for engine calibration, as the combustion process is carried out under real engine volume and boundary conditions, although these conditions are not entirely controlled or known.

On the other hand, the fundamental analysis through optically accessible test rigs have allowed the visualization of the combustion process in a simplified and nearly quiescent environment with controlled boundary conditions. Furthermore, larger optical access is available in comparison to an engine, easing the implementation of optical diagnostics. Thus, high-fidelity experiments can be performed, focusing on specific parameters to have a greater understanding of the topic of interest. Then, these results served as a valuable database to validate models through computational fluid dynamics, a tool that helps to reduce testing time and production costs.

Bazyn and Koci [13] analyzed the lift-off length for several jet spacing configurations in an optically accessible test rig with a large chamber volume compared to the space within an engine combustion chamber. They also found that, as the inter-jet spacing decreased, so did the lift off-length. Nevertheless, the authors found that these variations only appeared below a threshold proximity between jets (around 36°) whereas, for spacings above the threshold level, the sprays had a behavior similar to that of a single jet.

Although some investigations regarding the effect of inter-jet spacing on the combustion have been done, its influence is not entirely defined. Furthermore, most of the investigations were carried out in real diesel engines. In contrast, an optically accessible vessel with high-pressure and high-temperature capabilities is employed in this work, to study the combustion development under various inter-jet spacing configurations. This test rig is able to develop a nearly quiescent environment, while simulating the conditions found in the combustion chamber of current compression ignition engines in terms of temperature, pressure, and oxygen concentration.

In the following sections, the equipment used throughout the experiments is detailed, as well as the optical techniques employed. Then, the results obtained are described and discussed, followed by a statistical analysis. Finally, the main conclusions of the work are drawn.

Raul Payri, Jaime Gimeno, Marcos Carreres, Tomas Montiel; Understanding the effect of inter-jet spacing on lift-off length and ignition delay; Combustion and Flame, vol. 230, no. August, p. 111423, 2021. DOI: 10.1016/j.combustflame.2021.111423.

Nomenclature

ASOE	After start of energizing	ΔP	$P_{inj} - P_{back}$
ASOI	After start of injection	P_{back}	Back pressure
D_i	Inlet diameter	P_{inj}	Injection pressure
D_o	Outlet diameter	RSD	Relative standard deviation
ET	Energizing time	SSI	Second stage ignition
ID	Ignition delay	T	Temperature in the chamber
LOL	Lift-off length	θ	Inter-jet spacing
ρ	Density in the chamber	U_{th}	Theoretical velocity of the fuel
ρ_f	Density of the fuel		

2. Materials and methods

In the current section, a description of the equipment and methods used throughout the experiments is done.

2.1. Fuel delivery system

Initially, fuel is retrieved from a tank and sent through a purger to get rid of the air, followed by a filter to remove particles and impurities contained in the fuel. Then, the required combustible goes inside a CP3 pump, where its pressure is raised to the desired injection pressure and then sent to the common-rail, where it is contained. Thus, a relatively large volume of diesel fuel at high pressure is available to be delivered to the injector.

On the other hand, the excess of fuel coming out of the pump is sent back to the purger along with the excess fuel returning from the common rail. Before getting to the purger, the diesel fuel is directed through a heat exchanger, where its temperature is controlled.

2.2. Diesel injectors

The injectors employed throughout the experiments were the latest iteration of the piezo common-rail type 5 from Continental [14]. Both of them have

identical design, except for the distribution of the nozzle outlet holes. As they were specifically manufactured to study the jet to jet spacing, different outlet orifices configurations were established, which are depicted in Figure 1.

The nozzle of the injector 1v5 has an outlet hole to one side, which was taken as the reference isolated spray, and five holes to the other side with a spacing between jets of 30°, representing an injector of 12 equally distributed holes. On the other hand, the injector 3v3 has three holes on each side, in which one set has a jet spacing of 36 and the other of 45, emulating an injector with 10 and 8 holes, respectively. Both injectors can manage up to 250 MPa of injection pressure.

In this work, the sprays of interest are the ones enumerated and highlighted in dark orange, as these are the isolated spray and the sprays in the center of each configuration, ensuring the presence of neighbor jets. The outlet diameter of the holes of interest are presented in Table 1. The geometry of the injector was provided by the manufacturer.

Table 1: Geometry of the holes of interest.

Orifice	**1**	**2**	**3**	**4**
Outlet diameter [μm]	90.9	90.1	91.3	90.5

2.3. Test Rig and Optical Setup

2.3.1. High-Temperature and High-Pressure Test Rig

The injectors were employed in a high-pressure and high-temperature test rig, with an optically accessible combustion chamber with constant-pressure flow. This combustion chamber is able to reproduce real engine thermodynamic conditions, as it can reach temperatures and pressures up to 1100 K and 15 MPa, respectively. Additionally, the test rig has the attribute of maintaining nearly quiescent and steady conditions within the chamber, allowing to test a large range of boundary conditions and multiple repetitions without incurring

in alterations of the chamber conditions due to long testing periods [15, 16]. This test is rig thoughtfully detailed by Payri et al. [17].

The test rig has a frontal view to record the injector event of multi-orifice injectors, and two lateral views that can be used to observe the injection of single orifice injectors. As the study was done with multi-holes nozzles, the frontal view was employed.

2.3.2. MIE Scattering

Figure 2 depicts the optical setup used to measure the distance required by the spray to fully evaporate (liquid length) under non-reacting conditions employing the MIE-scattering imaging technique, widely used for the visualization of the liquid phase of the spray [18–20]. First, continuous light is provided by two 150 W quartz-halogen illuminators (Dolan-Jenner PL800), and directed to the sprays. Then, part of this light is reflected on the liquid droplets of the sprays, a process known as light scattering. Finally, the scattered light is captured by the high-speed camera (Photron FastCam SA-X2). Images were recorded at a frequency of 54 kfps, with an image resolution of 640 x 532 pixels, in which 6.24 pixels corresponded to 1 millimeter.

Even though it is not the main focus of the study, these measurements serve to partially characterize the behavior of the spray under non-reacting conditions and any alteration due to inter-jet spacing variations. Furthermore, these experiments allowed timing the start of injection, which is later useful to define the ignition delay after the start of injection (ASOI), instead of after the start of energizing (ASOE). In Figure 3, a representative sequence of the images recorded through this setup is depicted, and the algorithm employed to detect the liquid length is detailed by Payri et al. [21].

2.3.3. OH chemiluminescence*

During the combustion event, chemical reactions produce molecules in a transient high-energy state, which then move to a lower energy level emitting light during the process [22]. Formally, this process is known as chemilumines-

cence and can be used to track the ignition of the combustion. Specifically, CH radicals are considered to be appropriate markers of the cool flames or combustion first phase, whereas the appearance of OH radicals is used to characterize the second stage ignition (SSI), as they appear under high-temperature stoichiometric combustion [23]. Thus, the appearance of OH radicals can be used to measure the ignition delay [24], as the latter is typically defined as the time between the start of injection and the second stage ignition.

Moreover, OH radicals are found at the flame stabilization region on lifted and diffusive flames [25], and have the strongest light emittance band at 306 nm, which is considerably distant from most soot incandescence. Therefore, OH chemiluminescence is also considered as a reliable marker to measure lift-off length [26, 27].

Thus, it is possible to measure ignition delay and lift-off length through OH* chemiluminescence. To do so, the optical setup depicted in Figure 4 was employed.

First, the light emitted from the combustion reaches a dichroic mirror which mostly reflects UV radiation. Then, the reflected light goes through a narrow band-pass filter of 310 ± 5 nm to capture the desired emittance, a configuration extensively reported in the literature [16, 25, 28]. Finally, the light goes into a UV f/4 100 mm focal length lens connected to a high-speed image intensifier (Hamamatsu C10880), which is coupled to the high-speed camera (Photron FastCam SA5), where the image is recorded. Images were obtained at a frequency of 25 kfps and an image resolution of 736 x 320 pixels, where 4.39 pixels corresponded to one millimeter. An example of the images recorded through this setup is presented on Figure 5.

Then, the ignition delay is defined as the first moment in which the intensity level of the image surpasses the background noise of each injection event (Figure 5). On the other hand, the lift-off length is computed following the Engine Combustion Network guidelines [29]: first, the flame is divided through its axis into top and bottom profiles. Then, the peak of intensity along each profile is noted, and the lift-off length of each profile is calculated as the distance between

the nozzle tip and the first pixel with a value above 50% of the (previously calculated) maximum intensity. Then, both values are averaged into a final lift-off length value.

This process is done for every frame, and a time-dependent lift-off length is obtained as seen, for instance, in Figure 6. The observed is representative of the general trend seen throughout the measurements: Initially, a transient behavior is depicted as the lift-off gets closer to the nozzle tip, followed by a stable lift-off value during the injection period, and finalizing with the flame propagation after the end of injection (these steps can also be observed in Figure 5). Lastly, the lift-off length of the tested point is calculated as the mean of the lift-off length values contained in the steady region time frame.

2.3.4. Broadband chemiluminescence

In addition to the setup described in the previous section, broadband radiation of the flame was recorded with a high-speed camera (Photron FastCam SA-X2) equipped with a Zeiss 100 mm lens, as depicted in Figure 4. Images were taken with a frequency of 40 kfps and an image resolution of 1024x312 pixels, where 5.9 pixels were equivalent to one millimeter. Considering the spectral response of the camera, the light collected would mostly be due to the thermal radiation emitted from the soot particles, and any significant contribution from another type of chemiluminescence would only appear in low sooting flame cases [30]. Then, a qualitative evolution of the sooting flame can be obtained. This configuration was employed to detect any alteration, due to jet spacing variations, in the moment of appearance of soot particles. An example of the images recorded is presented in Figure 7, in which the soot detection moment is depicted.

2.4. Test Matrix

Boundary conditions such as injection pressure, chamber density and temperature were selected using guidelines from the Engine Combustion Network

(ECN) [29]. Injection conditions employed throughout the experiments are depicted in Table 2, in which every possible combination was employed.

Table 2: Test plan for each injector.

Parameter	Value	Units
Injection pressure	100 - 150 - 200	MPa
Chamber Temperature	800 - 900 - 1000	K
Chamber density	15.2 - 22.8 - 30.4	kg/m^3
Injection frequency	0.25	Hz
Energizing time	1.5	ms
Cycles per test point	10	-

2.5. Shot-to-shot dispersion

To reduce measuring errors and uncertainties, 10 cycles of each tested condition were measured. Afterward, all the repetitions results were averaged into a final value, and the relative standard deviation (RSD) was obtained for each measurement. The average RSD was 1.86% within the liquid length campaign, 3.8% for the lift-off length measurements, 4.13% for the ignition delay results and 3.32% for the soot appearance data. An illustrative example of the shot-to-shot dispersion of a tested point is presented in Figure 8. Nevertheless, the figures from the results section contain multiple tested point in a single plot, so the error bars were omitted to improve their readability.

3. Results and discussions

The following section details the phenomena observed throughout the measurements. First, the results from inert conditions are presented to observe the behavior of the spray in a non-reacting environment. Then, OH* chemiluminescence results are detailed, which serve to observe any variation in lift-off length and ignition delay due to inter-jet spacing variations. Additionally, soot appear-

ance delay for different inter-jet spacing values is discussed. Lastly, a statistical analysis of the lift-off length results is done.

3.1. Liquid length

Figure 9 depicts liquid length values for various boundary conditions of chamber temperature, chamber density, injection pressure and inter-jet spacing. It can be seen that the liquid length of the spray considerably decreases when the chamber temperature increases, as the larger enthalpy provided to the fuel droplets allows for a shorter evaporation distance. Likewise, an increment of the chamber density produces a reduction of the liquid length, as the rate of air entrainment is increased, reducing the distance required to fully evaporate.

Additionally, it is observed on Figure 10 that the injection pressure does not have a large influence on the liquid length: enlarging the injection pressure increases the fuel velocity but also decreases the fuel droplet size, which enhances the air entrainment. Thus, a balance is created in which the final evaporation distance is not greatly affected. The effects produced by the chamber temperature, density and injection pressure, have also been observed in [21, 31].

On the other hand, the results showed that variations of the inter-jet spacing did not have a particular impact on the liquid length values. Specifically, it can be seen that liquid length values remained mostly unaltered for inter-jet spacing values ranging from 120° (the isolated spray) to 30°. Thus, spray behavior was not affected by the inter-jet spacing in a non-reactive environment, in terms of the liquid length.

3.2. Lift-off length

The following results were obtained under a reacting environment, which is the main focus of this work as it is where the inter-jet spacing might have a larger influence. The values of lift-off length for several boundary conditions are depicted on Figure 11. The plots will initially separate both injectors, to improve their readability. On the left, the results of the injector 1v5 are depicted, whereas the right plot shows the lift-off length values of the injector 3v3, for the

same boundary conditions. The same methodology is also applied for Figure 12, which accounts for the influence of the injection pressure on the lift-off length.

It can be observed that the lift-off length is highly dependent on the chamber temperature and density. Specifically, an increase of the temperature or the density inside the chamber produced a reduction of the steady lift-off length, as the spay mixing process is enhanced. Additionally, Figure 12 depicts that an increase of the injection pressure generally produces a slightly larger lift-off length. These trends have been found by several authors [25, 28, 32], which serve to validate the consistency of the experiments of this work with well-known spray behavior.

Regarding the influence of the inter-jet spacing, considerable variations were found for different values of the jet-to-jet proximity. On the left plot of Figure 11 and Figure 12, it can be seen that, for every condition tested, the spray with inter-jet spacing of 30° had considerably lower lift-off length values than the isolated spray (or spray with 120° of spacing). Additionally, it can be observed that the differences were larger as the chamber density and temperature decreased, and the inter-jet spacing effect was predominant.

This trend was generally observed in the injector 3v3 as well, although smaller differences (or none, for some test points) were found between the sprays of study, which had more similar values of inter-jet spacing. Nevertheless, the spray with 36° of spacing from its neighbor jets, tended to have a slightly smaller lift-off length value than the spray with 45° of inter-jet spacing.

Lastly, both injectors results are merged into a single plot in Figure 13. On the inter-jet spacing, the trends commented on previous lines can be observed. It is depicted with more clarity that the spray with 30° of spacing had a lower lift-off length value than any of the other inter-jet spacing configurations, for each condition tested. On the other hand, sprays with an inter-jet spacing of 45° and 36° had similar lift-off length values (although slightly lower, generally) than that of the isolated spray, specially for lower temperatures. However, as the temperature increased, the reduction became more noticeable with values closer to that of the spray with inter-jet spacing of 30°, specially for the spray

with spacing of 36°

In this sense, the results showed that after certain proximity between sprays is reached (between 30° and 36°), the interaction between the sprays becomes a predominant factor in their behavior and the lift-off length is greatly reduced. Moreover, when the inter-jet spacing is greater than this threshold value (which varied slightly with the boundary conditions), the results are less distant to those obtained from the isolated spray (120° of spacing). Bazyn and Koci [13] studied the lift-off length for a range of 6 to 18 orifices nozzles, and noted a similar behavior to the results observed in this work. In particular, no significant variations were found up until the nozzle with 10 orifices (36° of spacing), in which the sprays began to be considerably affected by the neighboring plumes, shortening the lift-off length.

Then, the shortening of the lift-off length has been observed for sprays developing in a large test rig without interaction with a wall that could produce air re-entrainment and cause the shortening, as seen in the engine. The main plausible explanation for the observed change in behavior could be the interaction between combustion products of closely spaced jets. On this matter, Pickett et al. [33] conducted shadowgraphy imaging of reacting jet, revealing the presence of high-temperature reservoirs of combustion products and fresh ambient gas along the periphery of the spray. Moreover, Persson et al. [26] and Pickett et al. [33] proposed that the gas entrained by the jet is previously mixed with these high-temperature products, creating autoignition events near the nozzle that influence the lift-off length.

In this sense, the proportion of entrained hot combustion products and radicals could increase in closely spaced sprays [11]. Then, entrained gas at higher temperature could trigger autoignition near the nozzle, consequently reducing the lift-off length.

Other factors contributing to the observed results could be the radiative heat exchange occurring between the neighbor jets, which would be more intense as the sprays get closer to each other. Thus, the local temperature of the mixture could increase, accelerating the reactions and shortening the lift-off length, as

seen in Figure 13.

Lastly, the alteration of the fluid dynamics between the sprays as they get closer to each other. In this sense, various studies found that the fluid strain between sprays inhibits the ignition upstream of the lift-off length [34, 35]. A small inter-jet spacing could be affecting the fluid strain, allowing for ignition to occur closer to the orifice of the nozzle.

As this phenomenon was seen throughout the entire campaign and a large test matrix was employed, a statistical analysis of the observed results was done, which will be covered in detail in a later section.

3.3. Ignition delay

Ignition delay values for various boundary conditions are depicted in Figure 14 and Figure 15. Again, the results of both injectors are separated to improve readability and compare the same injection event. It can be seen that the ignition delay shortens with an increase of the chamber temperature, chamber density and injection pressure, as these phenomena enhance the air-fuel mixing process, accelerating the reactions and start of combustion. This behavior is expected and has also been described, for instance, by Pickett et al. [36] and Payri et al. [37].

Regarding the effect of the inter-jet spacing on the ignition delay, the results showed that, in general, the ignition delay was not considerably affected within the range of spacing distribution studied, which can also be seen with more clarity on Figure 16. Nevertheless, differences were observed at low temperature and density conditions, in which the spray with smaller inter-jet spacing had a slightly larger ignition delay. On the other hand, for more stable combustion boundary conditions, the ignition delay remained almost constant for each inter-jet spacing.

3.4. Initial soot appearance

To gain additional comprehension on the effect of inter-jet spacing on the combustion development after ignition, the initial soot appearance was obtained

through broadband chemiluminescence and compared to the start of ignition, captured with OH chemiluminescence Figure 17. As expected, the initial soot appearance followed the same trends as the ignition delay in which it shortens as the chamber temperature or chamber density increases, serving as a qualitative measurement of the combustion timing. Nevertheless, it can be seen that, for a given condition, the results obtained with OH chemiluminescence are constantly lower as OH radicals appear in the initial stages of the ignition process, the reason why OH chemiluminescence is preferred to obtain a quantitative ignition delay value [30].

Regarding the proximity between orifices it can be observed that, for a given boundary condition, the inter-jet spacing between sprays did not considerably delay or advance the initial soot appearance. Specifically, the initial appearance of soot after the start of combustion remained almost unaltered within the range of inter-jet spacing studied.

3.5. Statistical analysis

Based on the large test matrix employed throughout the measurements, the results observed were used to obtain a regression for the lift-off length. On this matter, the same approach used by Benajes et al. [28] is applied to characterize the lift-off length, so an exponential equation is employed:

$$LOL \propto T^a \cdot \rho^b \cdot {U_{th}}^c \cdot \theta^d \tag{1}$$

In which T refers to the chamber temperature, ρ to the chamber density, θ to the inter-jet spacing in degrees, and U_{th} to the theoretical velocity of the fuel at the nozzle exit, calculated by the equation[28]:

$$U_{th} = \sqrt{2\frac{\Delta P}{\rho_f}} \tag{2}$$

In which ΔP represents the difference between the injection pressure and the chamber pressure, and ρ_f the fuel density.

In Table 3, the coefficients obtained for the Equation 1 are presented. Additionally, the table contains the results obtained by Benajes et al. [28], Siebers and Higgins [38], for reference purposes.

Table 3: Coefficients obtained for the lift-off length correlation.

	a	b	c	d	e^*	R^2 [%]
Experimental data	-4.79	-0.83	0.71	0.81	-	94.1
Benajes et al. [28]	-3.89	-1	0.54	-	-1	99.5
Siebers and Higgins [38]	-3.74	-0.85	1	-	-1	-

* Influence of the oxygen concentration (not within the scope of this work).

It can be observed that the coefficients obtained with the experimental data have a general agreement with the values presented by Benajes et al. [28], Siebers and Higgins [38] in terms of chamber density, fuel velocity and chamber temperature, which has the largest impact on the lift-off length. Additionally, the high value of R^2 obtained confirms the repeatability and reliability of the results gathered. Moreover, the experimental data regression introduced a new variable that takes into account the effect of the spacing between sprays on the lift-off length.

As seen in previously presented results, the inter-jet spacing had a considerable effect in which as the spacing is reduced, so is the lift-off length value. The main physical mechanism producing this behavior could be the entrainment of hot combustion products near the nozzle, as detailed in the section of results and discussion of the lift-off length.

Finally, Figure 18 compares the experimental lift-off length values against the lift-off length obtained with the correlation, for each boundary condition. Overall, the correlation can reproduce the general behavior of the spray for the wide range of boundary conditions tested. However, a few points at the lowest condition of chamber temperature and density were under-estimated. This is in line with the higher instability noted at those test points due to poor boundary conditions for stable combustion, increasing the complexity in predicting the

behavior. Nevertheless, the general trend is represented, high accuracy being obtained for most operating conditions.

4. Summary and conclusions

This work studies the variation of the inter-jet spacing of a diesel injector, and its effect on the ignition delay and lift-off length of the spray. To do so, two multi-hole injectors were manufactured with outlet holes distributions that allowed to compare an isolated spray to another with an inter-jet spacing of 30°, during the same injection event. Additionally, the results were compared to the development of sprays with inter-jet spacing of 36° and 45°.

From the results obtained, the following main conclusions are drawn:

- In a non-reactive environment, the spray behavior was not affected for any of the tested values of inter-jet spacing, in terms of the liquid length.
- The measurements in reactive environment showed that after certain proximity between sprays is reached, the interaction between the sprays becomes a predominant factor in their behavior and the lift-off length is considerably reduced. Moreover, when the inter-jet spacing is greater than this threshold value, the results are less distant to those obtained from the isolated spray (120° spacing).
- An increase in the proportion of entrained hot combustion products and radicals by the closely spaced sprays was proposed as the main plausible explanation of the observed change in behavior. In this sense, entrained gas with a higher temperature could trigger autoignition near the nozzle, consequently reducing the lift-off length.
- The results obtained in the lift-off length were employed in a statistical analysis in which a novel regression for the lift-off length was developed, which accounted for the effect of the proximity between sprays.

– Regarding the ignition delay, small differences were only observed at low temperature and density conditions. For those conditions, the spray with smaller inter-jet spacing had a slightly larger ignition delay. Nevertheless, for more stable combustion boundary conditions, the ignition delay remained almost constant for each inter-jet spacing.

– An increase of the chamber temperature and density, considerably reduced the lift-off length and ignition delay. Moreover, enlarging the injection pressure slightly reduced the ignition delay and increased the lift-off length. These are well-known spray behavior, and served to validate the consistency of the experiments of this work.

References

[1] J. Claßen, S. Pischinger, S. Krysmon, S. Sterlepper, F. Dorscheidt, M. Doucet, C. Reuber, M. Görgen, J. Scharf, M. Nijs, S. C. Thewes, Statistically supported real driving emission calibration: Using cycle generation to provide vehicle-specific and statistically representative test scenarios for Euro 7, International Journal of Engine Research 21 (2020) 1783–1799. doi:10.1177/1468087420935221.

[2] R. A. Dobbins, R. A. Fletcher, B. A. Benner, S. Hoeft, Polycyclic aromatic hydrocarbons in flames, in diesel fuels, and in diesel emissions, Combustion and Flame 144 (2006) 773–781. doi:10.1016/j.combustflame.2005.09.008.

[3] M. Lapuerta, Á. Ramos, D. Fernández-Rodríguez, I. González-García, High-pressure versus low-pressure exhaust gas recirculation in a Euro 6 diesel engine with lean-NOx trap: Effectiveness to reduce NOx emissions, International Journal of Engine Research 20 (2019) 155–163. doi:10.1177/1468087418817447.

[4] C. Sayin, M. Gumus, M. Canakci, Influence of injector hole number on the performance and emissions of a di diesel engine fueled with biodiesel-

diesel fuel blends, Applied Thermal Engineering 61 (2013) 121–128. URL: http://dx.doi.org/10.1016/j.applthermaleng.2013.07.038. doi:10.1016/j.applthermaleng.2013.07.038.

[5] S. Lahane, K. A. Subramanian, Impact of nozzle holes configuration on fuel spray, wall impingement and NOx emission of a diesel engine for biodiesel-diesel blend (B20), Applied Thermal Engineering 64 (2014) 307–314. URL: http://dx.doi.org/10.1016/j.applthermaleng.2013.12.048. doi:10.1016/j.applthermaleng.2013.12.048.

[6] S. Han, J. Kim, C. Bae, Effect of air-fuel mixing quality on characteristics of conventional and low temperature diesel combustion, Applied Energy 119 (2014) 454–466. URL: http://dx.doi.org/10.1016/j.apenergy.2013.12.045. doi:10.1016/j.apenergy.2013.12.045.

[7] L. Y. Zhou, S. F. Dong, H. F. Cui, X. W. Wu, F. Y. Xue, F. Q. Luo, Measurements and analyses on the transient discharge coefficient of each nozzle hole of multi-hole diesel injector, Sensors and Actuators, A: Physical 244 (2016) 198–205. doi:10.1016/j.sna.2016.04.017.

[8] G. Aori, D. L. S. Hung, M. Zhang, Effect of Nozzle Configuration on Macroscopic Spray Characteristics of Multi-Hole Fuel Injectors Under Superheated Conditions, Atomization and Sprays 26 (2016) 439–462. doi:10.1615/AtomizSpr.2015011990.

[9] A. M. Rusly, M. K. Le, S. Kook, E. R. Hawkes, The shortening of lift-off length associated with jet-wall and jet-jet interaction in a small-bore optical diesel engine, Fuel 125 (2014) 1–14. URL: http://dx.doi.org/10.1016/j.fuel.2014.02.004. doi:10.1016/j.fuel.2014.02.004.

[10] M. K. Le, Y. Zhang, R. Zhang, L. Rao, S. Kook, Q. N. Chan, E. R. Hawkes, Effect of jet-jet interactions on soot formation in a small-bore diesel engine, Proceedings of the Combustion Institute 36 (2017) 3559–3566. URL: http://dx.doi.org/10.1016/j.proci.2016.07.025. doi:10.1016/j.proci.2016.07.025.

[11] C. Chartier, U. Aronsson, Ö. Andersson, R. Egnell, B. Johansson, Influence of jet-jet interactions on the lift-off length in an optical heavy-duty di diesel engine, Fuel 112 (2013) 311–318. doi:10.1016/j.fuel.2013.05.021.

[12] G. Lequien, E. Berrocal, Y. Gallo, A. Themudo E Mello, O. Andersson, B. Johansson, Effect of jet-jet interactions on the liquid fuel penetration in an optical heavy-duty di diesel engine, SAE Technical Papers 2 (2013). doi:10.4271/2013-01-1615.

[13] T. Bazyn, C. Koci, The Effect of Jet Spacing on the Combustion Characteristics of Diesel Sprays, in: THIESEL 2014 Conference on Thermo- and Fluid Dynamic Processes in Direct Injection Engines, 2014, pp. 1–19.

[14] R. Payri, P. Martí-Aldaraví, T. Montiel, A. Viera, Influence of aging of a diesel injector on multiple injection strategies, Applied Thermal Engineering 181 (2020) 115891. URL: https://doi.org/10.1016/j.applthermaleng.2020.115891. doi:10.1016/j.applthermaleng.2020.115891.

[15] M. Meijer, B. Somers, J. E. Johnson, J. D. Naber, S.-Y. Lee, L.-M. Malbec, G. Bruneaux, L. M. Pickett, M. Bardi, R. Payri, T. Bazyn, Engine Combustion Network (ECN): Characterization and comparison of boundary conditions for different combustion vessels, Atomization and Sprays 22 (2012) 777–806. URL: http://www.dl.begellhouse.com/journals/6a7c7e10642258cc,64b3d5d415f8eb91,0365a5274d55553b.html. doi:10.1615/AtomizSpr.2012006083.

[16] M. Bardi, R. Payri, L.-M. Malbec, G. Bruneaux, L. M. Pickett, J. Manin, T. Bazyn, C. L. Genzale, Engine Combustion Network: Comparison of Spray Development, Vaporization, and Combustion in Different Combustion Vessels, Atomization and Sprays 22 (2012) 807–842. URL: http://www.dl.begellhouse.com/journals/6a7c7e10642258cc,5b18f0e860ebc687,20adc8ff175d5f43.html. doi:10.1615/AtomizSpr.2013005837.

[17] R. Payri, J. Gimeno, S. Cardona, S. Ayyapureddi, Experimental study of the influence of the fuel and boundary conditions over the soot formation in multi-hole diesel injectors using high-speed color diffused back-illumination technique, Applied Thermal Engineering 158 (2019) 113746. URL: https://www.sciencedirect.com/science/article/pii/S1359431118378451?via{%}3Dihub. doi:10.1016/J.APPLTHERMALENG.2019.113746.

[18] R. Payri, J. S. Giraldo, S. Ayyapureddi, Z. Versey, Experimental and analytical study on vapor phase and liquid penetration for a high pressure diesel injector, Applied Thermal Engineering 137 (2018) 721–728. URL: https://doi.org/10.1016/j.applthermaleng.2018.03.097. doi:10.1016/j.applthermaleng.2018.03.097.

[19] F. Li, C. F. Lee, Z. Wang, Y. Pei, G. Lu, Impacts of duct inner diameter and standoff distance on macroscopic spray characteristics of ducted fuel injection under non-vaporizing conditions, International Journal of Engine Research (2020) 1–12. doi:10.1177/1468087420914714.

[20] J. S. Giraldo, R. Payri, P. Marti-Aldaravi, T. Montiel, Effect of high injection pressures and ambient gas properties over the macroscopic characteristics of the diesel spray on multi-hole nozzles, Atomization and Sprays 28 (2018) 1145–1160. URL: http://dl.begellhouse.com/journals/6a7c7e10642258cc,forthcoming,29651.html. doi:10.1615/AtomizSpr.2019029651.

[21] R. Payri, J. Gimeno, M. Bardi, A. H. Plazas, Study liquid length penetration results obtained with a direct acting piezo electric injector, Applied Energy 106 (2013) 152–162. URL: http://dx.doi.org/10.1016/j.apenergy.2013.01.027. doi:10.1016/j.apenergy.2013.01.027.

[22] A. G. Gaydon, The Spectroscopy of Flames, Springer Netherlands, 1974. URL: https://books.google.es/books?id=c77rCAAAQBAJ. doi:10.1007/978-94-009-5720-6.

[23] J. E. Dec, C. Espey, Chemiluminescence Imaging of Autoignition in a DI Diesel Engine, SAE Technical Paper 982685 (1998). doi:10.4271/982685.

[24] M. Jakob, T. Hülser, A. Janssen, P. Adomeit, S. Pischinger, G. Grünefeld, Simultaneous high-speed visualization of soot luminosity and OH * chemiluminescence of alternative-fuel combustion in a HSDI diesel engine under realistic operating conditions, Combustion and Flame 159 (2012) 2516–2529. URL: http://dx.doi.org/10.1016/j.combustflame.2012.03.004. doi:10.1016/j.combustflame.2012.03.004.

[25] B. Higgins, D. L. Siebers, Measurement of the Flame Lift-Off Location on DI Diesel Sprays Using OH Chemiluminescence, SAE Technical Paper 2001-01-0918 (2001).

[26] H. Persson, Ö. Andersson, R. Egnell, Fuel effects on flame lift-off under diesel conditions, Combustion and Flame 158 (2011) 91–97. URL: http://dx.doi.org/10.1016/j.combustflame.2010.07.020. doi:10.1016/j.combustflame.2010.07.020.

[27] A. J. Donkerbroek, M. D. Boot, C. C. Luijten, N. J. Dam, J. J. ter Meulen, Flame lift-off length and soot production of oxygenated fuels in relation with ignition delay in a DI heavy-duty diesel engine, Combustion and Flame 158 (2011) 525–538. URL: http://dx.doi.org/10.1016/j.combustflame.2010.10.003. doi:10.1016/j.combustflame.2010.10.003.

[28] J. Benajes, R. Payri, M. Bardi, P. Martí-aldaraví, Experimental characterization of diesel ignition and lift-off length using a single-hole ECN injector, Applied Thermal Engineering 58 (2013) 554–563. URL: http://www.sciencedirect.com/science/article/pii/S1359431113003153http://dx.doi.org/10.1016/j.applthermaleng.2013.04.044. doi:10.1016/j.applthermaleng.2013.04.044.

[29] ECN, Engine Combustion Network, Online, 2010. URL: www.sandia.gov/ecn/.

[30] J. V. Pastor, A. García, C. Micó, A. A. García-Carrero, Experimental study of influence of Liquefied Petroleum Gas addition in Hydrotreated Vegetable Oil fuel on ignition delay, flame lift off length and soot emission under diesel-like conditions, Fuel 260 (2020) 116377. URL: https://doi.org/10.1016/j.fuel.2019.116377. doi:10.1016/j.fuel.2019.116377.

[31] J. Manin, M. Bardi, L. M. Pickett, Evaluation of the liquid length via diffused back-illumination imaging in vaporizing diesel sprays, The Proceedings of the International symposium on diagnostics and modeling of combustion in internal combustion engines 8 (2012) 665–673. doi:10.1299/jmsesdm.2012.8.665.

[32] G. Lequien, Z. Li, O. Andersson, M. Richter, Lift-Off Length in an Optical Heavy-Duty Diesel Engine, SAE International Journal of Engines 8 (2015) 2015–24–2442. URL: http://papers.sae.org/2015-24-2442/. doi:10.4271/2015-24-2442.

[33] L. M. Pickett, S. Kook, H. Persson, Ö. Andersson, Diesel fuel jet lift-off stabilization in the presence of laser-induced plasma ignition, Proceedings of the Combustion Institute 32 (2009) 2793–2800. doi:10.1016/j.proci.2008.06.082.

[34] S. Chaudhuri, S. Kostka, M. W. Renfro, B. M. Cetegen, Blowoff dynamics of bluff body stabilized turbulent premixed flames, Combustion and Flame 157 (2010) 790–802. URL: http://dx.doi.org/10.1016/j.combustflame.2009.10.020. doi:10.1016/j.combustflame.2009.10.020.

[35] S. J. Shanbhogue, S. Husain, T. Lieuwen, Lean blowoff of bluff body stabilized flames: Scaling and dynamics, Progress in Energy and Combustion Science 35 (2009) 98–120. URL: http://dx.doi.org/10.1016/j.pecs.2008.07.003. doi:10.1016/j.pecs.2008.07.003.

[36] L. M. Pickett, D. L. Siebers, C. A. Idicheria, Relationship Between Ignition

Processes and the Lift-Off Length of Diesel Fuel Jets, SAE Paper 2005-01-3843 (2005). doi:10.4271/2005-01-3843.

[37] R. Payri, F. J. Salvador, J. Manin, A. Viera, Diesel ignition delay and lift-off length through different methodologies using a multi-hole injector, Applied Energy 162 (2016) 541–550. URL: http://linkinghub.elsevier.com/retrieve/pii/S0306261915013549. doi:10.1016/j.apenergy.2015.10.118.

[38] D. L. Siebers, B. Higgins, Flame Lift-Off on Direct-Injection Diesel Sprays Under Quiescent Conditions, SAE Technical Paper 2001-01-0530 (2001).

Acknowledgments

This work has been partially funded by Spanish Ministerio de Ciencia, Innovación y Universidades through project RTI2018-099706-B-100.

Tomas Montiel was supported by a research grant from Generalitat Valenciana and the European Social Fund (Reference: ACIF/2018/122).

Figures

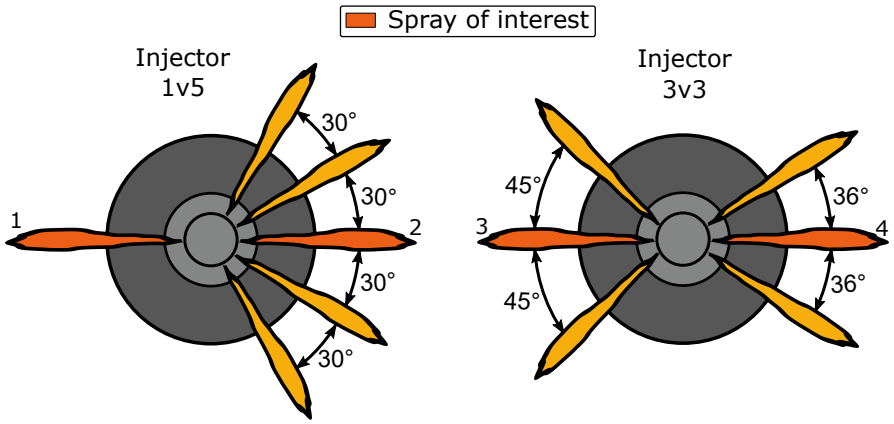

Figure 1: Outlet orifices configuration.

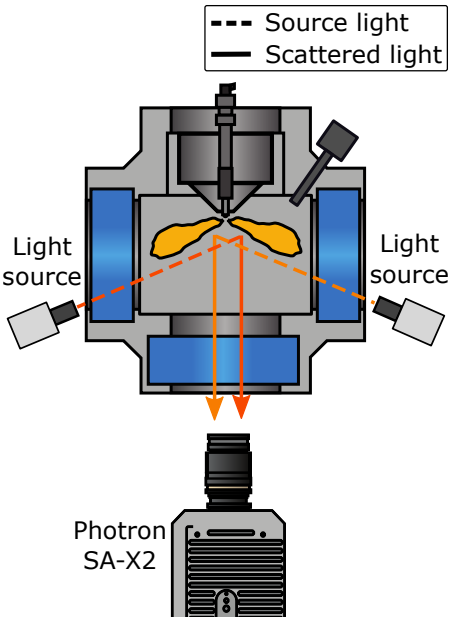

Figure 2: MIE-scattering optical setup.

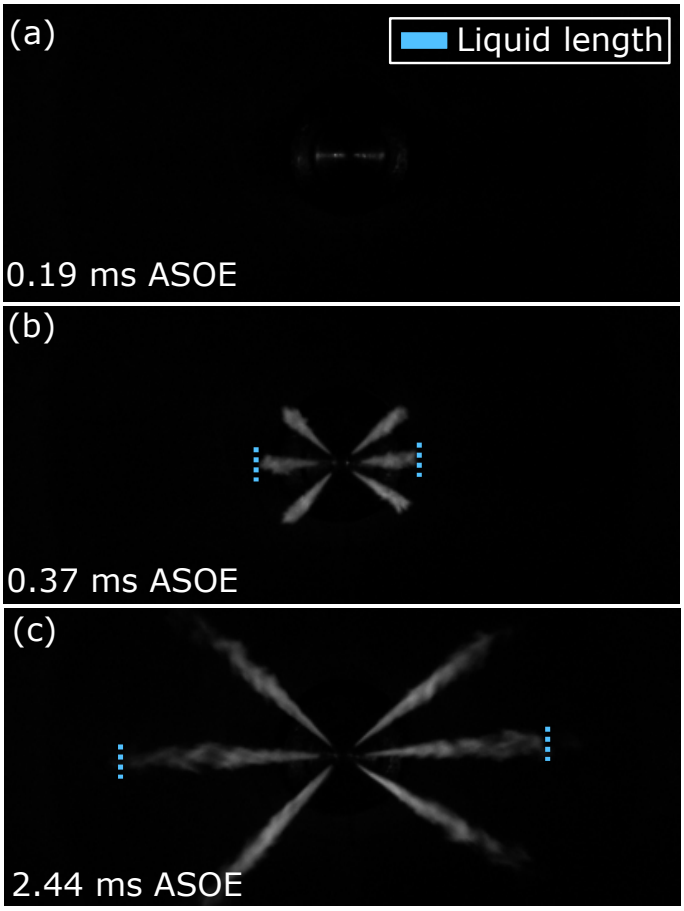

Figure 3: Liquid length sequence after start of energizing.

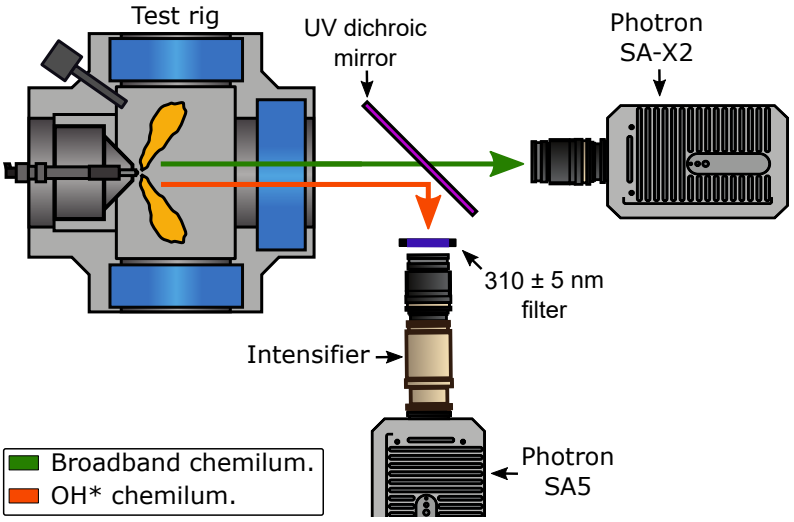

Figure 4: OH* and broadband chemiluminescence optical setup.

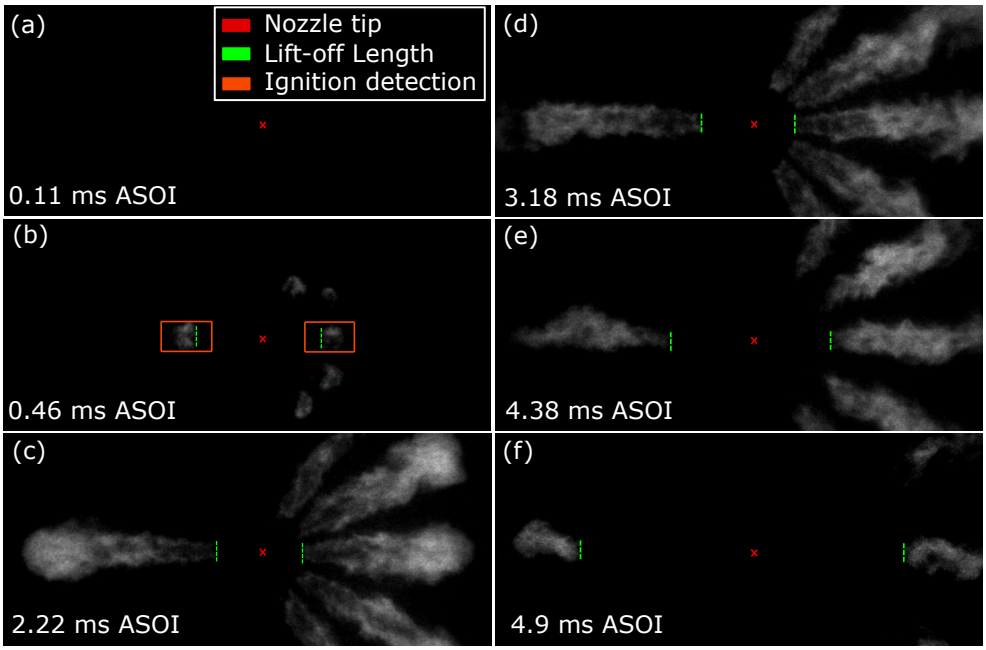

Figure 5: OH* chemiluminescence sequence after start of injection.

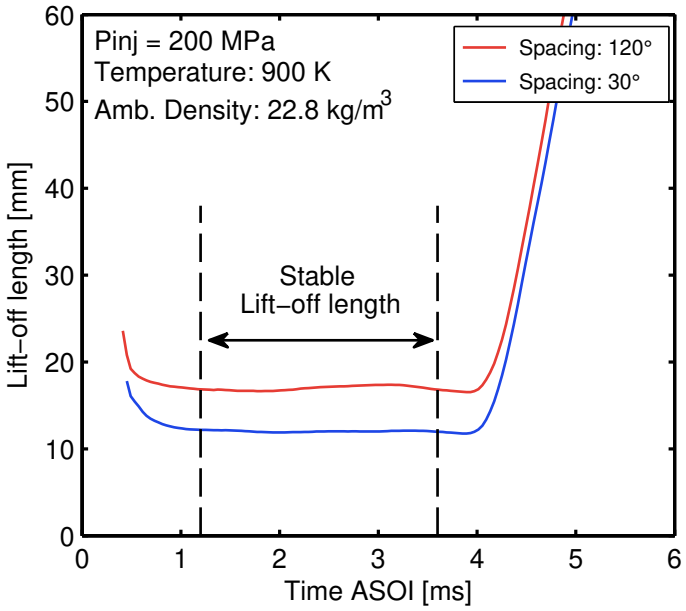

Figure 6: Lift-off length after start of injection.

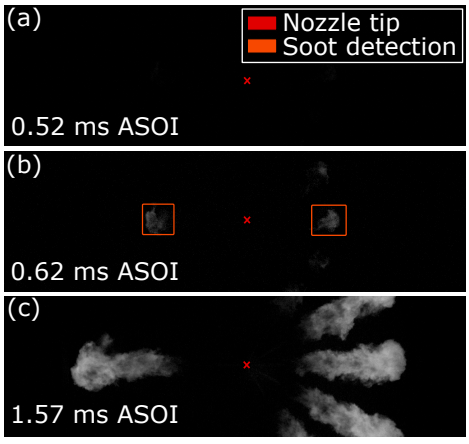

Figure 7: Broadband chemiluminescence sequence after start of injection.

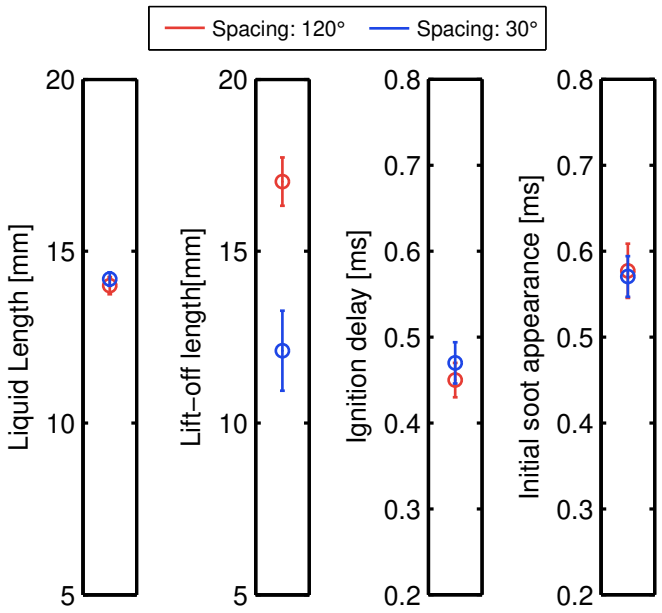

Figure 8: Shot-to-shot dispersion of a tested point. $P_{inj} = 200MPa, \rho = 22.8kg/m^3, T = 900K, injector : 1v5$.

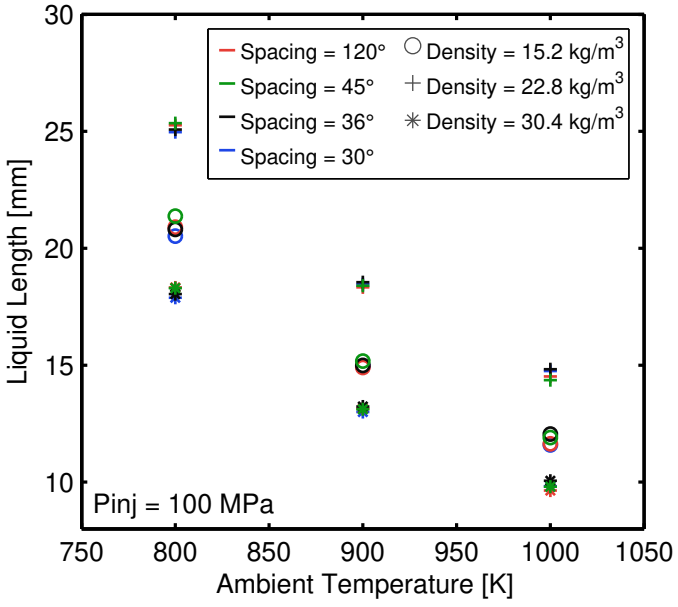

Figure 9: Liquid length variation for several values of inter-jet spacing, chamber temperature and chamber density.

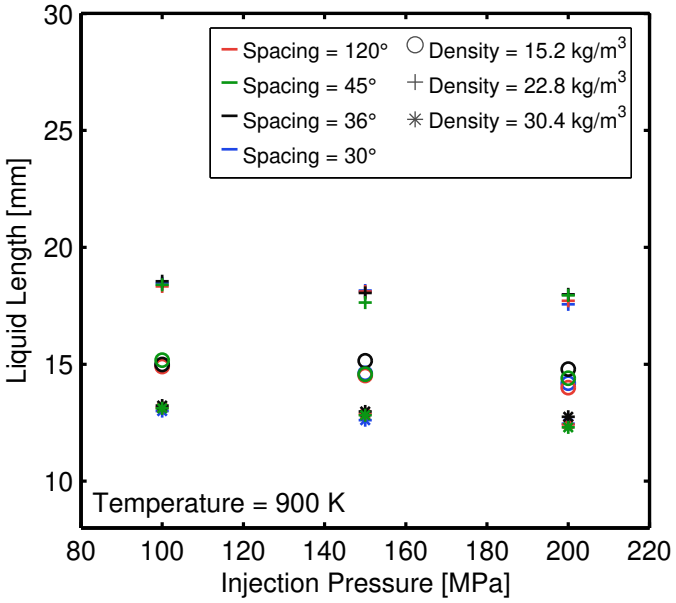

Figure 10: Liquid length variation for several values of inter-jet spacing, injection pressure and chamber density.

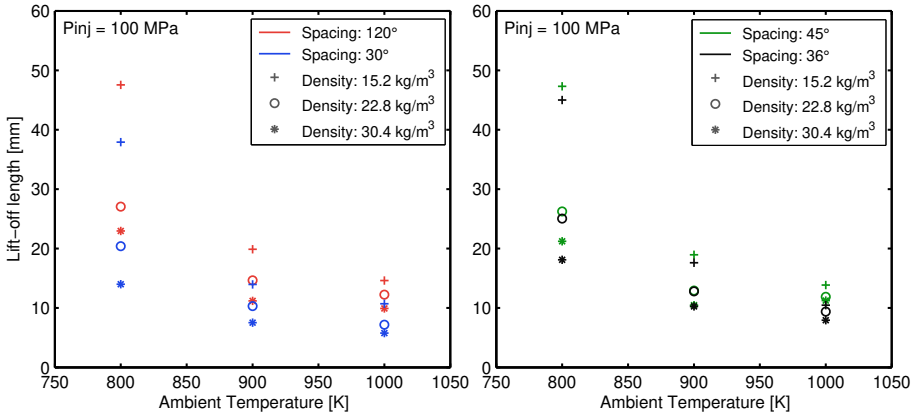

Figure 11: Lift-off length variation for several values of inter-jet spacing, chamber temperature and chamber density (left plot: 1v5 injector; right plot: 3v3 injector).

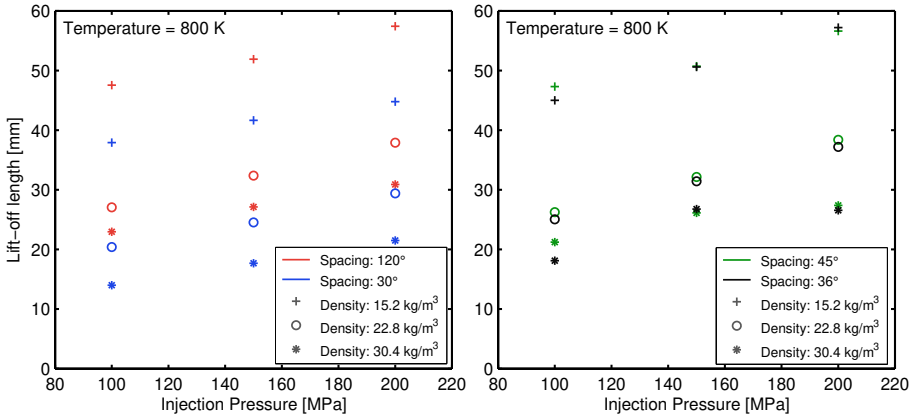

Figure 12: Lift-off length variation for several values of inter-jet spacing, injection pressure and chamber density (left plot: 1v5 injector; right plot: 3v3 injector).

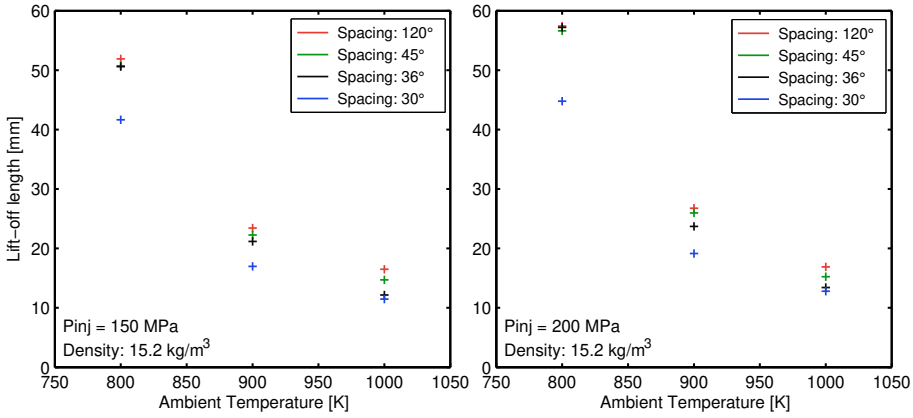

Figure 13: Lift-off length variation for several values of inter-jet spacing.

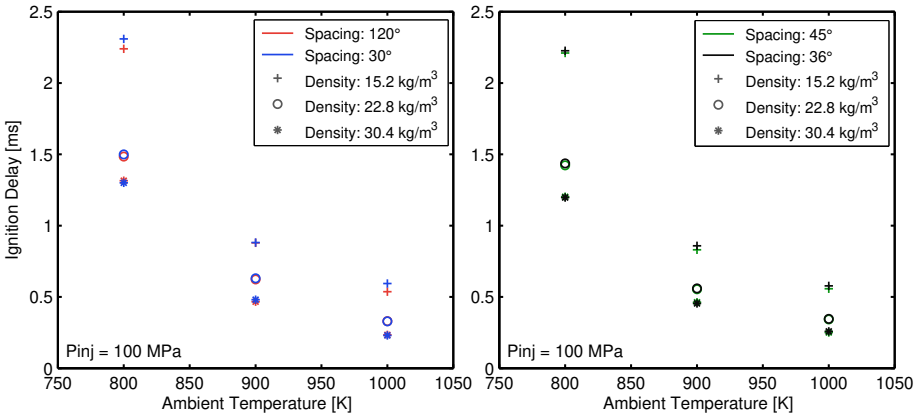

Figure 14: Ignition delay variation for several values of inter-jet spacing, chamber temperature and chamber density (left plot: 1v5 injector; right plot: 3v3 injector).

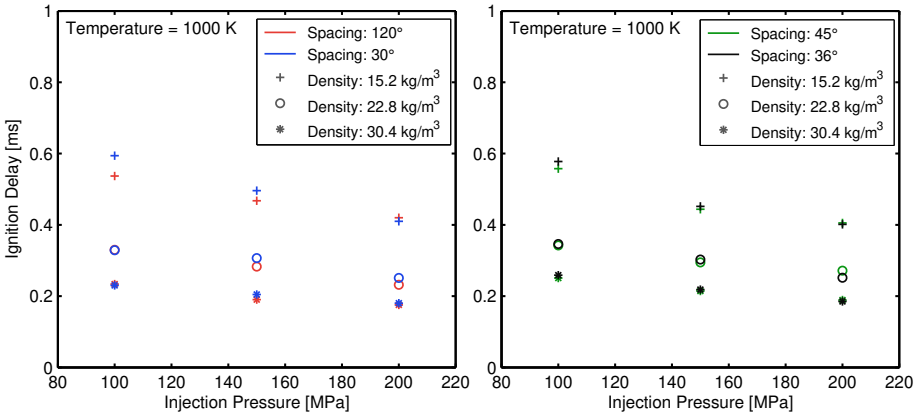

Figure 15: Ignition delay variation for several values of inter-jet spacing, injection pressure and chamber density (left plot: 1v5 injector; right plot: 3v3 injector).

Raul Payri, Jaime Gimeno, Marcos Carreres, Tomas Montiel; Understanding the effect of inter-jet spacing on lift-off length and ignition delay; Combustion and Flame, vol. 230, no. August, p. 111423, 2021. DOI: 10.1016/j.combustflame.2021.111423.

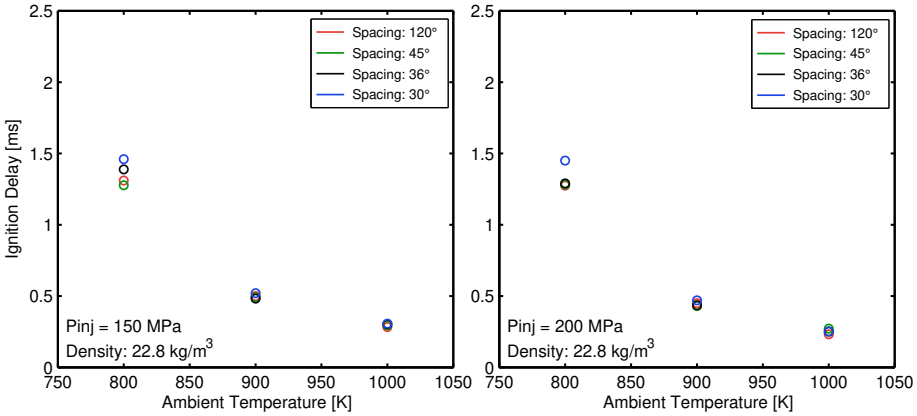

Figure 16: Ignition delay for several values of inter-jet spacing and chamber temperature.

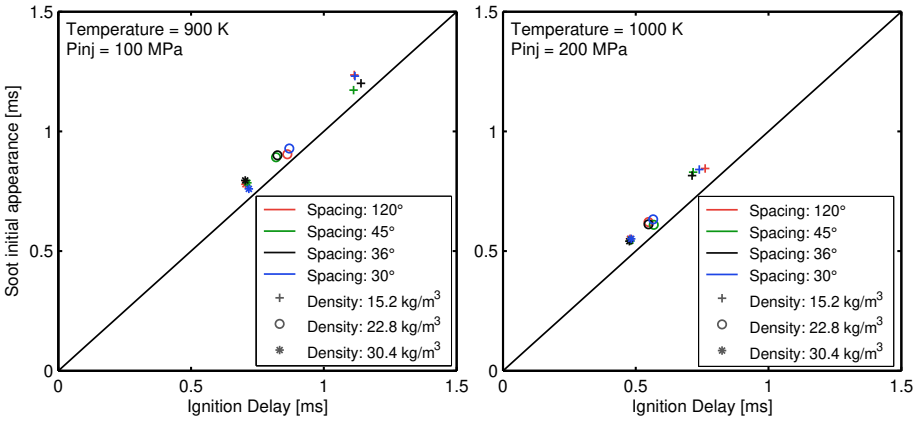

Figure 17: Initial soot appearance and ignition delay.

Raul Payri, Jaime Gimeno, Marcos Carreres, Tomas Montiel; Understanding the effect of inter-jet spacing on lift-off length and ignition delay; Combustion and Flame, vol. 230, no. August, p. 111423, 2021. DOI: 10.1016/j.combustflame.2021.111423.

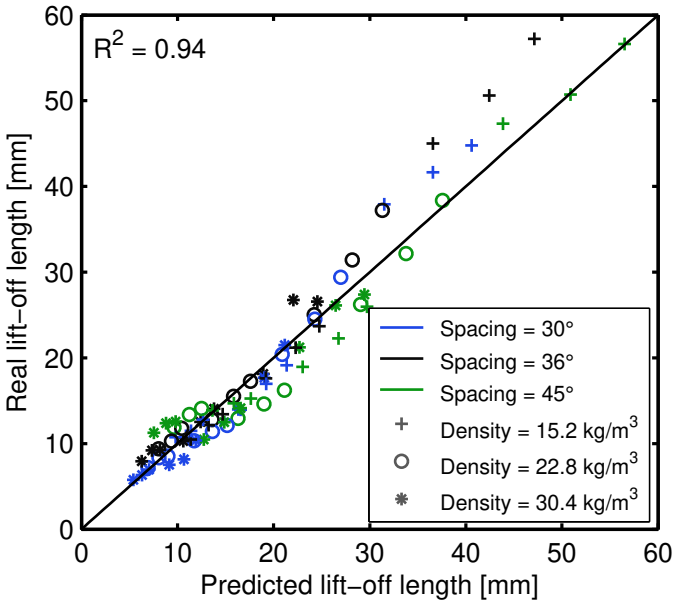

Figure 18: Experimental vs predicted lift-off length values.